

PACS numbers: 87.64.Cc; 87.85.Lf; 02.70.Uu
DOI: 10.1070/QE2014v044n07ABEH015481

A Monte Carlo based lookup table for spectrum analysis of turbid media in the reflectance probe regime

Xiang Wen, Xiewei Zhong, Tingting Yu, Dan Zhu

Abstract. **Fibre-optic diffuse reflectance spectroscopy offers a method for characterising phantoms of biotissue with specified optical properties. For a commercial reflectance probe (six source fibres surrounding a central collection fibre with an inter-fibre spacing of 480 μm; R400-7, Ocean Optics, USA) we have constructed a Monte Carlo based lookup table to create a function called getR(μ_a, μ_s'), where μ_a is the absorption coefficient and μ_s' is the reduced scattering coefficient. Experimental measurements of reflectance from homogeneous calibrated phantoms with given optical properties are compared with the predicted reflectance from the lookup table. The deviation between experiment and prediction is on average 12.1 %.**

Keywords: *optical fibres, diffuse reflectance, optical spectra, turbid media, Monte Carlo simulation.*

1. Introduction

After 20 years of development, near-IR spectroscopy has become an appealing tool for solving different analytical problems for all sorts of samples found in numerous fields, including food, agriculture, chemical, pharmaceuticals, textiles, polymers, cosmetics and medical [1–4]. Diffuse reflectance spectroscopy is an effective technique making it possible to obtain noninvasively information about optically related molecular components of turbid media. To quantitatively acquire the concentrations of spectral components, either a multivariate analysis method [5, 6] or a physical model based method [7, 8] can be employed. A multivariate analysis method relies on an empirical analysis model from spectra with known concentrations of each component, while a physical model 'recalculates' the reflectance at each wavelength to optical properties [absorption coefficient μ_a (cm^{-1}), reduced scattering coefficient μ_s' (cm^{-1})] and then determines the composition of a turbid medium from its optical properties. Compared to a multivariate analysis method, a physical model gives an insight to each spectrum component without any *a priori* representative set of spectra of the medium.

To create a physical model of the reflectance spectrum, the diffusion approximation [8], a semi-empirical analytical solution [9], an experiment-based lookup table (LUT) [7, 10] and a Monte Claro (MC) simulation based model [11, 12] have been proposed. Actually, the diffuse approximation is only suitable for multi-scattering events, but not available for the closely packed compact source and detection fibres [13]. Combining the diffuse approximation with phantom experiments, a semi-empirical analytical solution was developed which was valid for the case of short spacing between source and detection fibres [9]. But if the applicable range of optical properties was expanded, the accuracy of the approach was reported to need more parameters for calibration [14]. Thus, the experiment-based LUT becomes an alternative description for probe reflectance of different optical properties of turbid media [7]. The LUT was generated by measuring the reflectance of phantoms with known optical properties. However the accuracy of determining the optical property in this inverse modelling not only suffers from the finite number of phantoms, but also from the artifacts caused by phantom preparation and measurement. In contrast, the Monte Carlo (MC) simulation, as a gold standard of modelling, has been widely used to investigate complex systems and processes, validate approximate theoretical models and evaluate new techniques [15]. It can also be used for any probe design, and can analyse diffuse reflectance spectra [11, 12]. Although the initial simulation is time consuming, the resulting MC-based LUT can provide a rapid spectrum analysis. For such an MC-based LUT, it is necessary to consider the geometry of the fibre probe in the initial simulation, and the performance of the LUT should be tested in experiments.

Several investigators have constructed optical fibre probes consisting of a ring of six source fibres delivering white light, and a central collection fibre that brings light to a spectrally sensitive detector [7]. In this paper we use a commercially available probe (R400-7, Ocean Optics, USA); however, the procedure developed can be applied to any probe of similar construction. In this probe, the close spacing between the fibres (400 μm diameter of each fibre and a centre-to-centre distance of 480 μm) and the surrounding flange of metal supporting the fibres prevent the direct application of diffusion theory to predict the response of the probe to media with different optical properties. The probe geometry is different from previous works with Monte Carlo simulations [11, 12]. The specified MC simulation for the commercially available probe will give a wider possible application for spectrum analysis.

In this paper, an MC-based LUT was prepared and a function for interpolation of the LUT for particular values of the absorption coefficient μ_a and the reduced scattering coefficient μ_s' to yield the optical fibre probe reflectance, R, was developed. The reflectance of phantoms with different optical properties was measured to calibrate and verify the LUT.

Xiang Wen, Xiewei Zhong, Tingting Yu, Dan Zhu Britton Chance Center for Biomedical Photonics, Wuhan National Laboratory for Optoelectronics, Huazhong University of Science and Technology, Wuhan 430074, P.R.China; Key Laboratory of Biomedical Photonics of Ministry of Education, Department of Biomedical Engineering, Huazhong University of Science and Technology, Wuhan 430074, P.R. China; e-mail: dawnzh@mail.hust.edu.cn

Received 19 February 2014; revision received 20 March 2014
Kvantovaya Elektronika **44** (7) 641–645 (2014)
Submitted in English

2. Materials and methods

2.1. The profile of the fibre probe

The face of the optical R400-7 fibre probe (Ocean Optics, USA) is shown in Fi. 1. Six fibres in a circle deliver light from a halogen tungsten HL-2000 lamp source (Ocean Optics, USA) to the sample media and a central fibre collects reflected light from the sample media and delivers it to a USB-4000 spectrometer (Ocean Optics, USA). The diameter of all the fibres is $2r$ = 400 μm (NA = 0.22) and the centre-to-centre spacing between the source and detection fibres is d = 480 μm. A metal flange with a radius of 740 μm supports the fibres. The halogen tungsten lamp source provides a wide spectrum in visible and near-IR range. The spectrum in the range of 500–900 nm with a resolution of 1.5 nm (FWHM) is used for the analysis. All spectra are calibrated by a certified reflectance standard (SRS-99-020, Labsphere, USA). Calibration spectra are collected at a fixed distance (5 cm) above the standard.

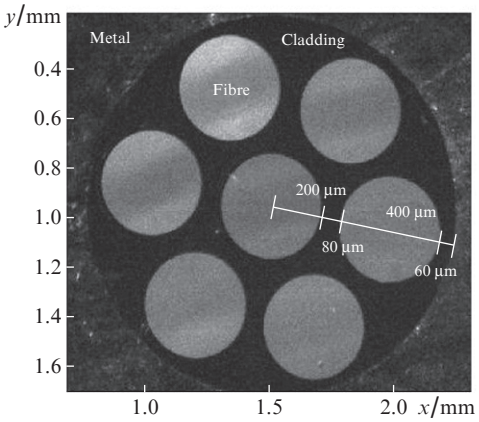

Figure 1. Face of the optical fibre probe. The diameter of all the fibres is 400 μm and the centre-to-centre spacing is 480 μm. The radius of the metal flange supporting the fibres is 740 μm.

2.2. Monte Carlo simulation for reflectance of the fibre probe

The details of the procedure for reflectance (R) simulation are described in [4]. In short, a GPU acceleration technique was adopted to reduce the simulation time [16], and CONV program by Wang et al. [17] was used to obtain diffuse reflectance [$R(r)$] based on the size of the source fibre. Then the reflectance was integrated across the detection fibre to determine the probability that a photon travelling a fixed distance would be collected (for the current probe's geometry). The simulated reflectance collected by the detection fibre (M_R, dimensionless), was determined by:

$$M_R = 6\int_{d-r}^{d+r} 2R(x)x\arccos\left(\frac{d^2+x^2-r^2}{2dx}\right)\mathrm{d}x, \qquad (1)$$

where the factor of 6 accounts for the six source fibres surrounding the detection fibre, R is the reflectance obtained after processing by the CONV program, d is the distance between the centres of the source and detector fibres and r is the radius of the fibre.

In Monte Carlo simulations, the number of simulated photons was 10^6; the reflectance index of the turbid media and the probe was 1.4 and 1.52, respectively; and the anisotropy factor was 0.7. In total, the reflectance of turbid media with 120 different combinations of μ_a and μ_s' was simulated for μ_a = 0.001–19.7 cm^{-1} and μ_s' = 0.3–614.4 cm^{-1}. The 2D matrix of simulated reflectance $R_s(\mu_a,\mu_s')$ on the log-log-log scale acts as a lookup table for returning the expected R-value of the fibre probe to a medium with given absorption and reduced scattering coefficients. The function getR(μ_a,μ_s'), using MATLAB language, returns the value of R_s for a choice of μ_a and μ_s'.

2.3. Calibration of the simulated spectrum with homogenous phantoms

Homogenous phantoms with different optical properties were made to calibrate the Monte Carlo simulation. The phantoms were made up of 20% intralipid (SichuanKelun Pharmaceutical Co., Ltd, China) and Indian ink (Solarbio, China). Three concentrations (20%, 5% and 1.25%) of intralipid scatterers and seven concentrations of India ink absorbers were used to create 21 phantoms. The absorption coefficient of all stock India ink solutions was measured with a high-accuracy spectrophotometer (Lambda 950, PerkinElmer, USA) before usage. To determine the optical properties of the

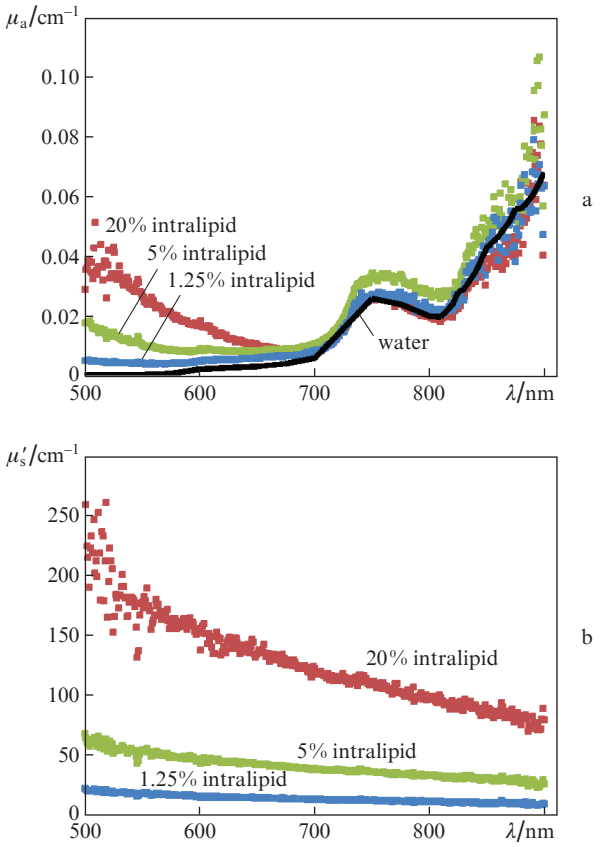

Figure 2. Optical properties of intralipid solutions measured by using the fluence rate in combination with the added absorber method: (a) absorption coefficients of three concentrations (20%, 5% and 1.25%) of intralipid solutions and water (data from [19]) and (b) scattering coefficients of the three concentrations of intralipid solutions.

phantoms we preliminary measured fluence by using the added absorber method [18]. The optical properties of intralipid in various concentrations are shown in Fig. 2. The absorption of the intralipid solution was primarily provided by water and lipid, and for the wavelength longer than 700 nm, the absorption was dominated by water. The calibration experiments showed a good match with published absorption coefficients of intralipid and water in the range from 700 to 1000 nm [19, 20].

The three concentrations of intralipid (20%, 5% and 1.25%) cover the scattering range of 8.11 to 260 cm^{-1}. Adding a 200 μL of stock India ink solution into 200 mL of each of the three intralipid solutions seven times resulted in a change in the absorption coefficients of the phantoms from 0.0032 to 31.6 cm^{-1}. After each addition, the reflectance of the phantom was added to the dataset $R_e(\mu_a, \mu_s')$. To have a better evaluation for the MC based LUT, only the spectrum between 600 and 800 nm was used (low noise level in Fig. 2).

Because the simulated reflectance R_s is normalised, it must be multiplied by a constant, K, before comparison with the measured reflectance. The equation

$$\chi = \sum \left[K \frac{R_s(\mu_a, \mu_s')}{R_e(\mu_a, \mu_s')} - 1 \right]^2 \qquad (2)$$

was used to extract the constant K, which minimised χ ($K = 10^{3.228}$).

2.4. Deviation between experimental and predicted results

The experimental measurements of reflectance, R_e, collected from homogeneous tissue phantoms with calibrated optical properties were compared with those predicted by the function $K\text{get}R(\mu_a, \mu_s')$. The relative deviation between the experiment and prediction was calculated as follows (D_{max} is the maximal deviation and D_{mean} is the mean deviation):

$$D_{max} = \max \left\{ \text{abs} \left[\frac{R_e(\mu_a, \mu_s') - K\,\text{get}R_s(\mu_a, \mu_s')}{R_e(\mu_a, \mu_s')} \right] \right\}, \qquad (3)$$

$$D_{mean} = \text{mean} \left\{ \text{abs} \left[\frac{R_e(\mu_a, \mu_s') - K\,\text{get}R_s(\mu_a, \mu_s')}{R_e(\mu_a, \mu_s')} \right] \right\}. \qquad (4)$$

3. Results

3.1. Monte Carlo simulation for reflectance of the fibre probe

Figure 3 illustrates the distribution of light fluence rates and reflectance after Monte Carlo simulations. The source fibre is centred at $x = 0.048$ cm, $y = 0$ cm, while the detector fibre is centred at $x = 0$ cm, $y = 0$ cm. Figure 3a shows the fluence rate $F(x, z)$ at $y = 0$ (in W cm^{-2} per 1 W delivered or in cm^{-2}). Figure 3b shows the escaping reflectance $R(x, y)$ (in cm^{-2}). These two figures correspond to the case of medium-to-low scattering. The light spreads out broadly, extending beyond the collection fibre. If scattering increases, light concentrates around the collection fibre, and the measured signal from the probe increases. Figure 3c and 3d show the $F(x, z)$ and $R(x, y)$ for the case of a high scattering coefficient, illustrating how high scattering restricts the light around the source fibre and

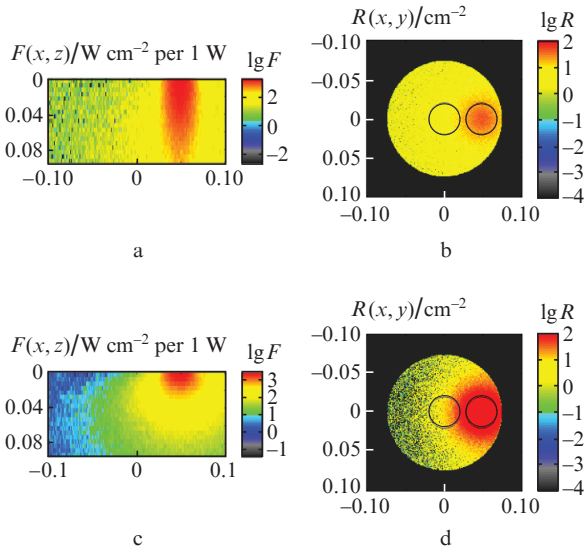

Figure 3. Monte Carlo simulation for the measured reflectance of the probe: (a, c) fluence rate $F(x, z)$ (in W cm^{-2} per 1 W delivered) in the plane passing through centres of the fibres ($\mu_a = 0.729$ cm^{-1}) and (b, d) local reflectance $R(x, y)$ (in cm^{-2}). The central black circle indicates the collecting fibre and the black circle centred at $x = 0.048$ cm indicates the source fiber at (a, b) moderate ($\mu_s' = 969$ cm^{-1}) and high ($\mu_s' = 153.60$ cm^{-1}) scattering of tissue.

prevents light from reaching the collection fibre. Thus, a further increase in scattering will decrease the detected light.

3.2. MC-based LUT for spectrum analysis

Figure 4a shows the lookup tables created by MC simulations for media with various optical properties. The LUT was constructed in logarithmic coordinates, representing $\lg KR_s$ versus $\lg\mu_a$ and $\lg\mu_s'$ (all the optical properties have the same dimension: cm^{-1}). The position labelled by A corresponds to the case of Figs 3a and 3b, with low-to-medium scattering. As in the experiment based LUT, when the scattering is small and increases, the light concentrates closer to the centre and the number of photons reaching the collection fibre increases. Hence, the gradient $\partial(KR_s)/\partial\mu_s'$ is positive. The position labelled by B corresponds to the case of Figs 3c and 3d, with high scattering. If scattering further increases, the light concentrates more around the source fibre and the number of photons reaching the collection fibre decreases. Hence, the gradient $\partial(KR_s)/\partial\mu_s'$ is negative. Figure 4b shows experimental probe reflectance on tissue phantoms. Because of a small number of phantoms the range of the optical properties of the experiment based LUT is not as large as the MC based LUT. Nevertheless, the same tendency for the changing the reflectance with the μ_a and μ_s' is observed. When absorption increases, the probe reflectance decreases. When scattering increases, the fiber probe reflectance first increases, reaches a maximum at $\mu_s' = 10^{1.5}$–$10^{2.0}$ and then decreases. The deviations between Monte Carlo simulations and measurements in phantom experiments D(%) are plotted in Fig. 4c. For the measured range of optical properties, the interpolation from $\text{get}R(\mu_a, \mu_s')$ matches well with experiment measurements with an average deviation of 12.1%, and the range of the deviation is from 0 to 44.7%.

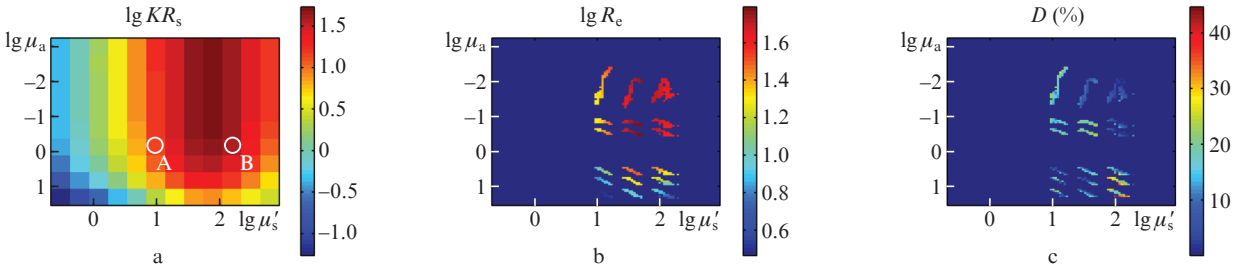

Figure 4. (a) Monte Carlo based LUTs for the measured reflectance of the fbre probe, (b) measured spectra of reflectance from calibrated phantoms of biotissue and (c) deviation between the LUP interpolation and the experimental spectra.

4. Discussion

When analysing the reflectance spectrum collected by the probe with closely packed source and collection fibres, the LUT of reflectance can be constructed by either using the results of the experiments on tissue phantoms or Monte Carlo simulation. Compared with the experimental LUT, the simulated one has several advantages. Firstly, the number and precision of the data in the simulated LUT can be set reasonably according to the demand of the spectrum analysis. However, for turbid media the data distribution more depends on the natural spectral property of the medium components. Secondly, the anisotropic factor in MC simulations can be adjusted according to the scattering property of the media to be analysed. And the greatest advantage of the Monte Carlo simulation is the spectrum sensitivity for the probe that can be predicted in the stage of probe design, which gives reference information about the probe reflectance response to the variation of absorption and scattering properties. Nevertheless, much more attention should be paid to the fact that the deviation between the simulated and experimental reflectance is highly related to the experimental error and the fitting parameter, K.

From the Monte Carlo based LUT and experimental results (Fig. 4), we can find that for the same absorption coefficient, the measured reflectance of the medium measured by the probe is not monotonic if reduced scattering can vary from low to very high values. The probe reflectance will reach a maxim when reduced scattering coefficients lie in the range from $10^{1.5}$ to 10^2 cm^{-1}. Some previous semi-empirical analytical solutions based on measurements of low scattering media assume a monotonic relation between probe reflectance and scattering coefficients [9, 21]. This will induce wrong spectra analysis results when the scattering of the media is higher than 100 cm^{-1}.

The LUT specifies the relationship between the μ_a and μ_s' of a homogeneous medium and the reflectance signal acquired by the Ocean Optics probe with fibres 400 μm in diameter. There are loci of μ_a and μ_s' values which give the same reflectance signal. When reflectance at multiple wavelengths is collected in a reflectance spectrum and basic functions for spectral components within a homogeneous medium are known, the least-squares method can approximate the contribution of each of the spectral components, by recreating μ_a and μ_s' at the measured wavelengths and by predicting a spectrum using the reflectance from the LUT for the values of μ_a and μ_s'. Comparing experimental and predicted spectra allows the least-squares fitting to be conducted and the concentration of each spectrum components to be derived. But for a heterogeneous tissue like skin, the spectral components are distributed in layers. The analysis for its spectral components requires a modified functional model to approach the multilayered spectrum to a homogenous model or build a higher dimension LUT with optical properties of each layer of skin.

5. Conclusions

We have presented a Monte Carlo based lookup table for the spectrum analysis of homogenous media. A function for the interpolation of the LUT for particular values of the absorption coefficient μ_a and the reduced scattering coefficient μ_s' to yield the optical fibre probe reflectance, R, is developed. Experimental measurements of the reflectance collected from homogeneous tissue phantoms with calibrated optical properties are compared with the measurements predicted by the function. The deviation between the experiment and prediction is on average 12.1%. The LUT has shown a monotonic decrease in reflectance with increasing absorption coefficients and a nonmonotonic dependence of reflectance on the scattering coefficients for the probe in question. The LUT is useful for spectrum analysis of homogeneous media and expands the application of diffuse reflectance spectrum. The function can be directly used for the commercial probe and the protocol can be a reference to the LUT construction for any similar optical fibre probe.

Acknowledgements. The authors express their gratitude to Prof. Steven Jacques at Oregon Health and Science University, USA for his help.

This study was supported by the grants of the National Nature Science Foundation of China (Grant Nos 81171376, 91232710, 812111313), the Science Fund for Creative Research Group (Grant No. 61121004), and the Research Fund for the Doctoral Programme of Higher Education of China (Grant No. 20110142110073).

References

1. McClure W.F. *J. Near Infrared Spectrosc.*, **11**, 487 (2003).
2. Cao J., Sharma S. *ISRN Textiles*, **2013**, 649406 (2013).
3. Pojic M.M., Mastilovic J.S. *Food Bioprocess Tech.*, **6**, 330 (2013).
4. Zhong X., Wen X., Zhu D. *Opt. Express*, **22**, 1852 (2014).
5. Viscarra Rossel R.A., Walvoort D.J.J., McBratney A.B., Janik L.J., Skjemstad J.O. *Geoderma*, **131**, 59 (2006).
6. Borin A., Ferrão M.F., Mello C., Maretto D.A., Poppi R.J. *Anal. Chim. Acta*, **579**, 25 (2006).
7. Rajaram N., Nguyen T.H., Tunnel J.W. *J. Biomed. Opt.*, **13**, 050501 (2008).
8. Tseng S.H., Hayakawa C., Tromberg B.J., Spanier J., Durkin A.J. *Opt. Lett.*, **30**, 3165 (2005).
9. Zonios G., Dimou A. *Opt. Express*, **14**, 8661 (2006).

10. Nichols B.S., Rajaram N., Tunnel J.W. *J. Biomed. Opt*., **17**, 057001 (2012).
11. Karlsson H., Fredriksson I., Larsson M., Stromberg T. *Opt. Express*, **20**, 12233 (2012).
12. Palmer G.M., Ramanujam N. *Appl. Opt.*, **45**, 1062 (2006).
13. Finlay J.C., Foster T.H. *Med. Phys*., **31**, 1949 (2004).
14. Zonios G., Dimou A. *Biomed. Opt. Express*, **2**, 3284 (2011).
15. Zhu D., Lu W., Zeng S., Luo Q. *J. Biomed. Opt*., **12**, 064004 (2007).
16. Jiang C., He H., Li P., Luo Q. *J. Innov. Opt. Health Sci*., **5**, 1250004 (2012).
17. Wang L., Jacque S.L., Zheng L. *Comput. Meth. Prog. Bio*., **54**, 141 (1997).
18. Martelli F., Zaccanti G. *Opt. Express*, **15**, 486 (2007).
19. Hale G.M., Querry M.R. *Appl. Opt*., **12**, 555 (1973).
20. Michels R., Foschum F., Kienle A. *Opt. Express*, **16**, 5907 (2008).
21. Zonios G., Dimou A. *Opt. Express*, **17**, 1256 (2009).